

# Crystal-poor versus crystal-rich ignimbrites: A competition between stirring and reactivation

Christian Huber<sup>1</sup>, Olivier Bachmann<sup>2</sup>, and Josef Dufek<sup>1</sup>

<sup>1</sup>School of Earth and Atmospheric Sciences, Georgia Institute of Technology, 311 Ferst Drive, Atlanta, Georgia 30332, USA

<sup>2</sup>Department of Earth and Space Sciences, University of Washington, Seattle, Washington 98195, USA

## ABSTRACT

**Ignimbrites, providing unique windows into magma reservoirs prior to explosive volcanic eruptions, are of two main types: (1) crystal-rich dacites, and (2) dominantly crystal-poor rhyolites. Crystal-rich dacites are typically homogeneous, while crystal-poor ignimbrites can display strong gradients in composition and crystallinity. This presents a conundrum, as the more viscous, crystal-rich units should be less prone to stirring and mixing. As ignimbrites typically erupt following a reheating event induced by recharge from below, this dichotomy reflects the competition between two time scales: (1) a thermal reactivation time scale that measures the time necessary to make a locked crystal mush rheologically eruptible (<50% crystals), and (2) a homogenization time scale associated with convective stirring. Using a well-constrained thermo-mechanical model of a magma reservoir, we show that the reactivation time scale of locked mushes is much greater than the time necessary to homogenize reservoirs by convective stirring. Hence, crystal-rich units, which require a reactivation stage, are inevitably well stirred. In contrast, crystal-poor magmas are rheologically ready to be mobilized without reactivation and need not be thoroughly mixed prior to eruption. This model provides an integrated picture of upper crustal reservoirs and has major implications for the link between shallow plutonic and volcanic rocks.**

## INTRODUCTION

Two major types of explosive silicic volcanic deposits (referred to as ignimbrites) are preserved in long-lived continental arcs: the chemically homogeneous crystal-rich monotonous intermediates, and the typically chemically zoned, but largely crystal-poor, ash-flow sheets (Table 1; Hildreth, 1981; Bachmann et al., 2002; Bachmann and Bergantz, 2008). The monotonous intermediates are nearly identical in composition to the average upper continental crust, with a dacitic composition of ~68 wt% SiO<sub>2</sub> (Bachmann et al., 2002). Zoned ignimbrites have compositionally highly evolved caps (crystal-poor, high-SiO<sub>2</sub> rhyolite) and typically grade into less silicic compositions. In some instances (e.g., Bishop Tuff; Hildreth, 1981), the whole-rock difference in SiO<sub>2</sub> between early and late erupted material is only a few percent, while in other cases (e.g., Carpenter Ridge Tuff

and Nelson Mountain Tuff in Colorado, United States; Lipman, 2007), the late-erupted stratigraphic levels have compositions resembling those found in the monotonous intermediates (dacite to mafic dacite; SiO<sub>2</sub> ~10 wt% lower than in the crystal-poor cap).

The contrast between these two types of deposits is illustrated in Figure 1 and Table 1 using well-documented examples in the Southern Rocky Mountain volcanic field. This dichotomy is striking when considering the viscosity of the progenitor magmas for the different cases. Magma (melt + crystals) mixture viscosity is very sensitive to the volume fraction of crystals present (Einstein, 1906; Marsh, 1981; Dingwell et al., 1993). Particularly puzzling is the fact that the monotonous intermediates, despite being the most viscous magma produced on Earth (Scaillet et al., 1998), are noticeably homogeneous at the hand-sample scale (Bachmann et al., 2002).

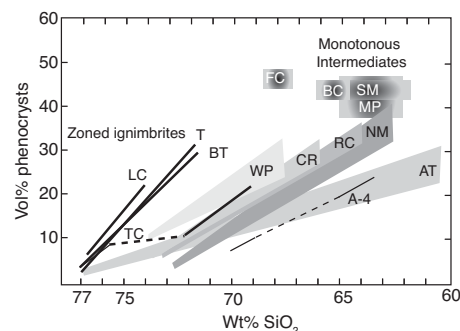


**Figure 1. Variations in SiO<sub>2</sub> and crystal contents for ignimbrites in western United States (LC—Lava Creek Tuff; T—Tshigere Member of Bandelier Tuff; BT—Bishop Tuff; TC—Tiva Canyon Tuff; WP—Wason Park Tuff; CR—Carpenter Ridge Tuff; RC—Rat Creek Tuff; NM—Nelson Mountain Tuff; AT—Ammonia Tanks Tuff; FC—Fish Canyon Tuff; BC—Blue Creek Tuff, SM—Snowshoe Mountain Tuff; MP—Masonic Park Tuff) and Japan (A-4). Modified from Hildreth (1981); data from Hildreth (1981) and Lipman (2000, 2006). Plot shows unzoned monotonous intermediates and zoned units grading into them.**

In contrast, dominantly crystal-poor ignimbrites, sourced from magmas with lower crystallinities, are often, but not always, zoned in composition, crystallinity, and temperature (e.g., Hildreth, 1981). We propose the following scenario to explain these two types of ignimbrites (Fig. 2):

- The crystal-rich monotonous intermediates are reactivated crystal mushes. Upper crustal reservoirs attain high crystallinities (>50 vol% crystals) fairly rapidly (Huber et al., 2009), without necessarily attaining chemical homogeneity. They become locked (not able to undergo whole-chamber convection) due to the presence of a continuous crystal framework (Marsh, 1981). In order to erupt, these magmas must be unlocked by partial melting in response to new inputs of hot magma (e.g., underplating recharge events), as evidenced by resorption textures of many mineral phases they contain (Bachmann et al., 2002).
- Dominantly crystal-poor magmas are not locked by any crystal framework, and do not need any reactivation period to erupt, although they frequently record a thermal pulse prior to eruption (e.g., Wark et al., 2007; Molloy et al., 2008).

TABLE 1. IGNIMBRITES FROM THE SOUTHERN ROCKY MOUNTAIN VOLCANIC FIELD (LIPMAN, 2006)

Name	Age (Ma)	Volume (km <sup>3</sup> )	SiO <sub>2</sub> (wt%)		Crystallinity (%)	
			Bottom	Top	Bottom	Top
Snowshoe Mountain Tuff	26.87	>500	62–66	62–66	40–45	40–45
Nelson Mountain Tuff	26.9	>500	74	63	<10	25–40
Cebolla Creek Tuff	26.9	250	61–64	61–64	35–40	35–40
Rat Creek Tuff	26.91	150	74	65	<10	30
Wason Park Tuff	27.38	>500	72	63	10	30
Blue Creek Tuff	27.2	250	64–66	64–66	40–45	40–45
Carpenter Ridge Tuff	27.55	>1000	74	66	3	30
Fish Canyon Tuff	28.02	5000	66–68	66–68	40–50	40–50
Masonic Park Tuff	28.3	500	62–65	62–65	35–45	35–45

In such a scenario, time scales of (1) mush reactivation (unlocking the crystalline skeleton) and (2) stirring of a dominantly liquid batch of magma that contains chemical and/or thermal heterogeneities compete to form the erupted deposit. We predict that if the reactivation time scale is much longer than the stirring time scale, any magma chamber than had to undergo reactivation will be largely homogeneous by the time it erupts.

## PHYSICAL MODEL

### Convection and the Stirring Time Scale

The stirring time is defined as the time necessary to reduce the length scale of heterogeneities in the convecting fluid (here, a magma body) to dimensions where diffusion takes over as the most efficient homogenization process (Huber et al., 2009). The stirring time depends on the rate of strain accumulation in the convective body:

$$t_m = \frac{1}{2\dot{\epsilon}} \log\left(\frac{\dot{\epsilon}L^2}{D}\right), \quad (1)$$

where  $\dot{\epsilon}$  is the mean Lagrangian strain rate,  $L$  is the thickness of fluid convecting, and  $D$  is the diffusion coefficient that is expected to control further homogenization (Coltice and Schmalzl, 2006). The strain rate is a function of the Rayleigh number,  $Ra = DrgL^3/(\mu\kappa)$ .

$$\dot{\epsilon} = a \frac{\kappa}{L^2} Ra^b, \quad (2)$$

where we use  $a = 0.023$  and  $b = 0.685$  from three-dimensional (3-D) temperature-dependent viscosity calculations (Coltice and Schmalzl, 2006),  $\kappa$  is the thermal diffusivity of the magma, and  $\mu$  is viscosity. Using such a correlation between strain rate and  $Ra$ , Huber et al. (2009) showed that, irrespective of the temporal evolution of convection ( $Ra$  varying with time), a convective body requires 5–10 overturns to be stirred efficiently.

The strength of the source of buoyancy in a convecting magma body controls the rate of strain accumulation, and therefore the stirring time. The dominant buoyancy sources in a convecting magma body are crystal plume-driven convection and buoyant gas exsolved from underlying intrusion (Bergantz and Ni, 1999; Ruprecht et al., 2008). A large accumulation of strain and homogenization of the magma reservoir depends on the duration over which buoyant materials (e.g., bubbles or crystal plumes) are formed and/or injected in the magma body. In the calculations shown in Figure 3, we assume a constant source of buoyancy. Although more complex volatile or

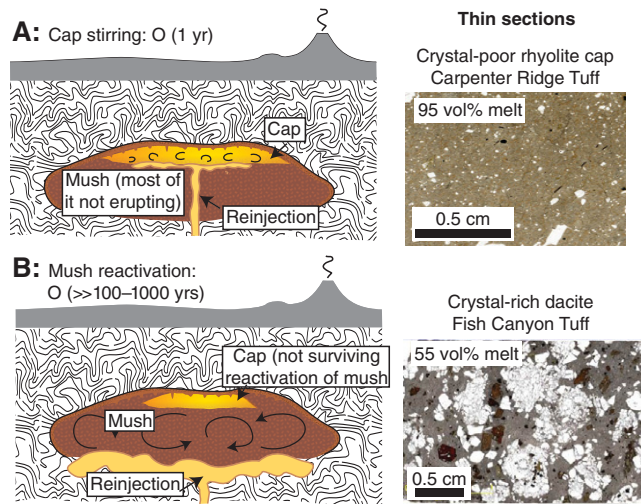


**Figure 2.** Left: Schematic illustrations of erupted cap versus erupted mush in world of ignimbrites. Right: Photomicrographs of thin sections from two typical ignimbrites from central San Juan volcanic field (Colorado, United States); zoned Carpenter Ridge Tuff (~1000 km<sup>3</sup>), and unzoned Fish Canyon Tuff (~5000 km<sup>3</sup>), erupted ~500 k.y. apart from same area.

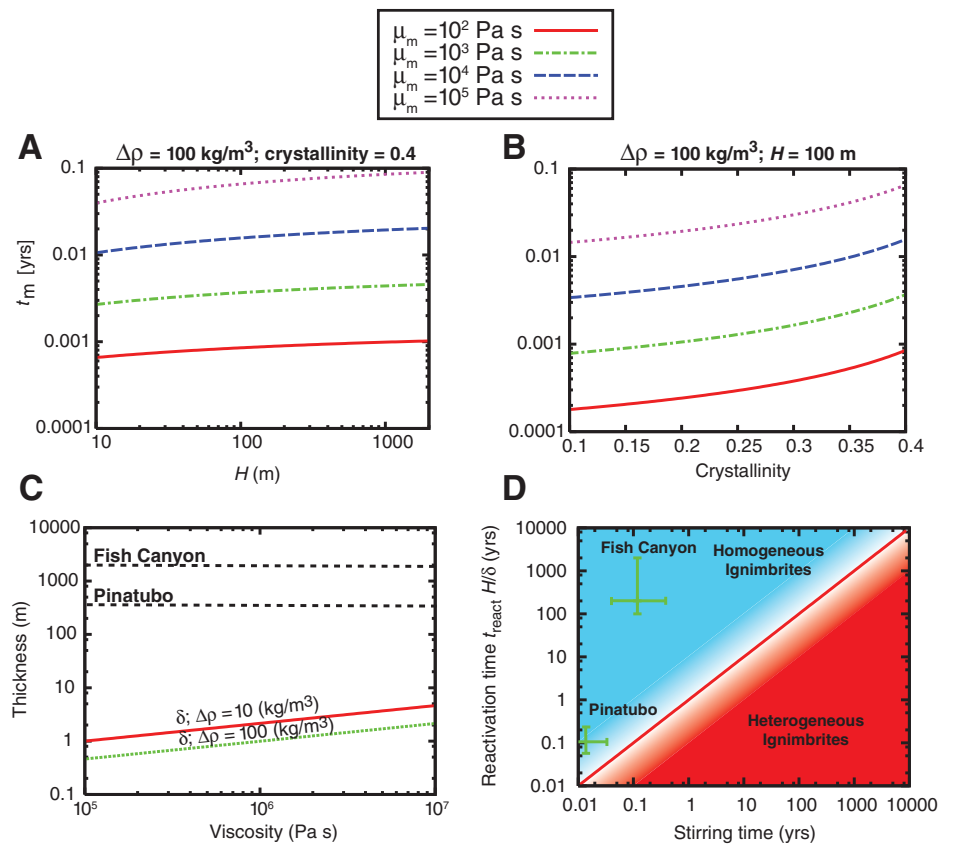


**Figure 3.** Stirring and reactivation time scales. **A:** Stirring time,  $t_m$ , versus thickness of convecting fluid,  $H$ , for different melt viscosities. Crystallinity is fixed at 0.4 and buoyancy is  $\Delta\rho = 100 \text{ kg/m}^3$ . **B:** Stirring time as function of magma's average crystallinity for different melt viscosities and buoyancy source  $\Delta\rho = 100 \text{ kg/m}^3$ . **C:** Comparison between critical boundary layer thickness for different magma bulk viscosities and thickness of two reactivated dacitic mushes, Pinatubo (from eruption of 15 June 1991) and Fish Canyon magma, Colorado (ca. 28 Ma). Thickness of reactivated magma bodies is estimated from erupted volume, geophysical data (Pinatubo), and size of observed caldera (Fish Canyon Tuff). **D:** Comparison between stirring and reactivation times; we used lower bound  $t_{\text{react}} H/\delta$  and equation 1 (see text) to estimate two time scales for Fish Canyon Tuff and data of Pallister et al. (1992) for 1991 eruption of Pinatubo. When reactivation time exceeds stirring time, ignimbrite is expected to be homogeneous (blue shaded region). Two examples (Pinatubo and Fish Canyon Tuff) are well within homogeneous regime. Two data points are lower bound estimates and error bars provide reasonable time scales. Effect of crystallinity on rheology of magma is calculated from Hess and Dingwell (1996), assuming critical crystallinity of 0.5.

crystallization scenarios are possible, the short calculated stirring times (Fig. 3) indicate that volatile flux from underlying cooling intrusions can remain roughly constant over these time scales and provide a sufficient amount of potential energy to stir the convective magma capping them.

Using a source of buoyancy that corresponds to a plausible value for bubble-driven or crystal-driven convection ( $\Delta\rho = 100 \text{ kg/m}^3$ ; see the GSA Data Repository<sup>1</sup>), the stirring time remains  $\ll 1 \text{ yr}$  for most choices of magma body thickness  $L$  and magma viscosity (Fig. 3). The stirring time depends only weakly on the thickness of the fluid layer to homogenize due to the fact that  $\text{Ra}^b/L^2 \sim L^{0.055}$  with the correlation for the strain rate of Coltice and Schmalzl (2006). The main controls on the stirring time for a magma body are the mixture viscosity of the fluid (Figs. 3A and 3B) and the strength of the buoyancy force responsible for convection. For example, the definitions above imply a variation of stirring time of a factor of  $\sim 5$  for any order of magnitude of  $\Delta\rho$  or  $\mu$ .

### Reactivation Time Scale for Crystal Mushes

The reactivation time is defined as the period between the onset of an intrusive phase of hot magma underneath a shallow crystal mush and the time at which the mush is fully open (capable of being drained from the magma chamber for a large eruption). The reactivation time strongly depends on (1) the size and average crystallinity of the mush, (2) the size, frequency, and configuration of magma intrusions carrying the enthalpy required to open the mush (Dufek and Bergantz, 2005; Annen and Sparks, 2002), and (3) the tectonic setting (phase assemblage of both mush and recharge, including their volatile contents; Huber et al., 2010a, 2010b).

As we seek a measure of reactivation time scale that does not depend on intrusion size, intrusion emplacement frequency, and mush size, we introduce a reactivation time scale that corresponds to the time required to unlock the mush over the critical boundary layer thickness  $\delta$  required to start convection:

$$\delta = \left( \frac{\kappa\mu\text{Ra}_{\text{cr}}}{\Delta\rho g} \right)^{1/3}, \quad (3)$$

where  $\kappa$ ,  $\mu$ , and  $\Delta\rho$  are, respectively, the thermal diffusivity, the dynamic viscosity of the magma, and the density contrasts responsible

for the convective motions.  $\text{Ra}_{\text{cr}}$  is the critical Rayleigh number at which convection starts ( $\sim 10^3$ ). After this time scale, convection is expected to start stirring the reactivated part of the mush. Prior to the onset of convection, the heat transfer is diffusive and the melting front  $H(t)$  in the mush (i.e., the thickness of reactivated mush) progresses on average as  $H(t) = c \cdot t^{1/2}$ , where  $c$  is a constant that depends on the phase diagram of the mush and on the latent heat of fusion of the mineral species that melt. The reactivation time scale,  $t_{\text{react}}$ , becomes

$$t_{\text{react}} = \frac{1}{c^2} \left( \frac{\kappa\mu\text{Ra}_{\text{cr}}}{\Delta\rho g} \right)^{2/3}, \quad (4)$$

where the constant  $c \approx 4 \text{ m/yr}^{1/2}$  was determined from the calculations of Huber et al. (2010b; 2011) for dacitic mushes and andesitic intrusions.

As the critical boundary layer thickness is usually small for most magmas (on the scale of meters; see Fig. 3C), in most situations it will be much smaller than the thickness of mush. This choice of length and time scale is advantageous as it is independent of assumptions of the total mush size and of the frequency of emplacement of new intrusions ( $t_{\text{react}} \ll \text{frequency of intrusion}^{-1}$ ). In addition, this time scale provides a lower bound on the time required to rejuvenate a mush,  $t_{\text{react,minimum}} \approx H t_{\text{react}}/\delta$ , where  $H$  is the mush thickness (see Fig. 3C). The mush/boundary layer thickness ratio,  $H/\delta$ , is typically 100–1000. This approximation assumes that the frequency of injection is such that the temperature at the intrusion-mush boundary and the speed of the advancing melting front in the mush remain roughly constant throughout the reactivation process. Such conditions will overestimate the melting efficiency of the mush as the heat transfer will decrease when the melting front moves away from the intrusion, and will underestimate even more the time scale of reactivation. The objective is, however, to estimate the minimum possible rejuvenation time scale for all given assumptions, which is important when we compare this time scale against mixing time scales.

### DISCUSSION

Based on our calculations (Figs. 3C and 3D), we obtain values of  $t_{\text{react,minimum}}$  that range from about half a year for a mush thickness of a few hundred meters (e.g., Pinatubo dacite; Pallister et al., 1992) to a few hundred years for the thickest mushes ( $\sim 2\text{--}5 \text{ km}$ , Fish Canyon magma; Bachmann and Bergantz, 2006). We emphasize that these are crude underestimates of the effective reactivation time, especially for large crystal mushes, where it can be as much as 1–2 orders of magnitude greater than these

estimates. Nevertheless, our half-year estimate for the 1991 Pinatubo eruption is close to the lower bound estimation of 10 weeks, from April to the eruption of the crystal-rich dacite on 15 June, a time scale inferred from seismicity and phreatic explosions (Pallister et al., 1992).

The degree of homogeneity of erupted volcanic deposits is often attributed to the efficiency and duration of convective mixing (stirring) of the magma prior to the eruption. We find that in most relevant cases, where the buoyancy source for stirring is large due to gradients in crystallinity or exsolved volatile content, the time required to homogenize a magma body to the scale of hand samples is relatively short (years or less). When compared to the time required to reactivate a locked crystal mush by new injections of hot magmas, even using lower bound estimates for the rejuvenation time scales, the stirring time is at least two orders of magnitude shorter for large magma bodies. We therefore conclude that the dichotomy between homogeneous crystal-rich ignimbrites and crystal-poor rhyolites to crystal-rich dacites can be explained by the presence or absence of a mush reactivation stage (Fig. 4):

- Crystal-poor magmas can be erupted shortly after the injection of new magma, before enough strain is accumulated for homogenization. They are therefore commonly heterogeneous (although they do not need to be; see Dunbar et al., 1989).
- In contrast, crystal-rich ignimbrites are inherently homogeneous because of the strain accumulated by convective stirring during the protracted reactivation episode. This model reconciles both types of ignimbrites and provides a coherent framework of upper crustal magma reservoirs, linking large volcanic deposits and upper crustal plutons, which dominantly represent fully crystallized mushes.

### ACKNOWLEDGMENTS

Huber was supported by a Swiss National Science Foundation postdoctoral fund; Bachmann was supported by U.S. National Science Foundation (NSF) grant EAR-0809828; and Dufek was supported by NSF grant EAR-0948532. We thank Guil Gualda, Jim Beard, and an anonymous reviewer for constructive criticism on an earlier version of this manuscript.

### REFERENCES CITED

- Annen, C., and Sparks, R.S.J., 2002, Effects of repetitive emplacement of basaltic intrusions on thermal evolution and melt generation in the crust: *Earth and Planetary Science Letters*, v. 203, p. 937–955, doi:10.1016/S0012-821X(02)00929-9.
- Bachmann, O., and Bergantz, G.W., 2006, Gas percolation in upper-crustal silicic crystal mushes as a mechanism for upward heat advection and rejuvenation of near-solidus magma

<sup>1</sup>GSA Data Repository item 2012021, supplemental material, is available online at [www.geosociety.org/pubs/ft2012.htm](http://www.geosociety.org/pubs/ft2012.htm), or on request from editing@geosociety.org or Documents Secretary, GSA, P.O. Box 9140, Boulder, CO 80301, USA.

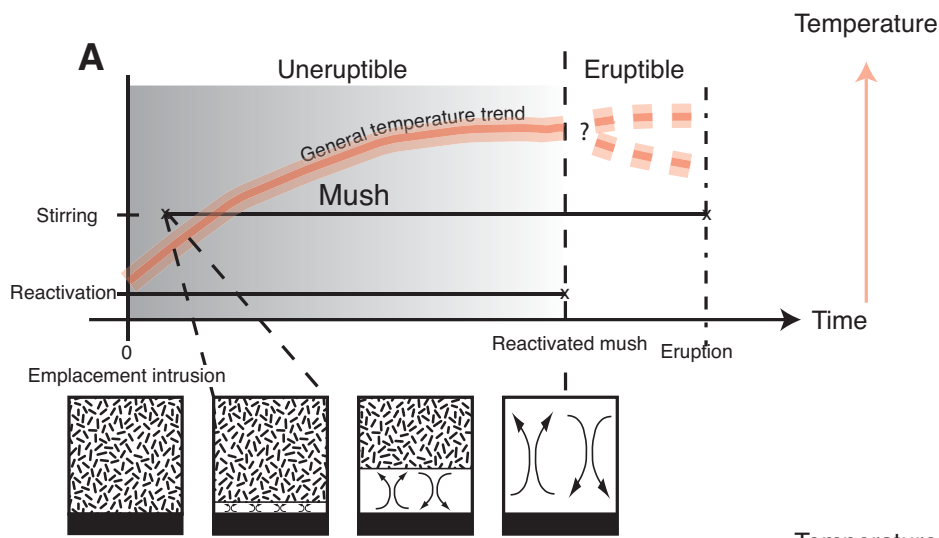
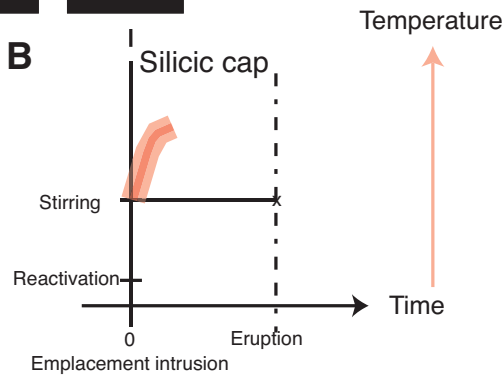


**Figure 4. Schematic illustration of dichotomy between crystal-poor and crystal-rich silicic ignimbrites in terms of temporal evolution. The y axis shows two different time scales (stirring and reactivation) effective over different parts of evolution of mushes and crystal-poor silicic magmas. Duration for reactivation of crystal mushes greatly exceeds stirring time. Magma therefore becomes more homogeneous as reactivation proceeds and reaches deeper in the mush. We expect that largest mushes will become more homogeneous. Crystal-poor silicic magmas (e.g., silicic caps) are not locked as intrusions are emplaced; they can therefore erupt soon after large intrusion is emplaced, before being efficiently homogenized by stirring.**



bodies: *Journal of Volcanology and Geothermal Research*, v. 149, p. 85–102, doi:10.1016/j.jvolgeores.2005.06.002.

Bachmann, O., and Bergantz, G.W., 2008, Deciphering magma chamber dynamics from styles of compositional zoning in large silicic ash flow sheets, in Putirka, K.D., and Tepley, F.J., eds., *Minerals, inclusions and volcanic processes: Reviews in Mineralogy and Geochemistry*, v. 69, p. 651–674, doi:10.2138/rmg.2008.69.17.

Bachmann, O., Dungan, M.A., and Lipman, P.W., 2002, The Fish Canyon magma body, San Juan volcanic field, Colorado: Rejuvenation and eruption of an upper crustal batholith: *Journal of Petrology*, v. 43, p. 1469–1503, doi:10.1093/petrology/43.8.1469.

Bergantz, G.W., and Ni, J., 1999, A numerical study of sedimentation by dripping instabilities in viscous fluids: *International Journal of Multiphase Flow*, v. 25, p. 307–320, doi:10.1016/S0301-9322(98)00050-0.

Coltice, N., and Schmalzl, J., 2006, Mixing times in the mantle of the early Earth derived from 2-D and 3-D numerical simulations of convection: *Geophysical Research Letters*, v. 33, L23304, doi:10.1029/2006GL027707.

Dingwell, D., Bagdassarov, N., Bussod, G., and Webb, S.L., 1993, Magma rheology, in Luth, R.W., ed.,

Experiments at high pressure and applications to Earth's mantle: *Mineralogical Association of Canada Short Course 21*, p. 131–196.

Dufek, J., and Bergantz, G.W., 2005, Lower crustal magma genesis and preservation: A stochastic framework for the evolution of basalt-crust interaction: *Journal of Petrology*, v. 46, p. 2167–2195, doi:10.1093/petrology/egi049.

Dunbar, N.W., Kyle, P.R., and Wilson, C.J.N., 1989, Evidence for limited zonation in silicic magma systems, Taupo Volcanic Zone, New Zealand: *Geology*, v. 17, p. 234–236, doi:10.1130/0091-7613(1989)017<0234:EFLZIS>2.3.CO;2.

Einstein, A., 1906, Eine neue Bestimmung der Molekuldimensionen: *Annals of Physics*, v. 19, p. 289–306, doi:10.1002/andp.19063240204.

Hess, K.U., and Dingwell, D.B., 1996, Viscosities of hydrous leucogranite melts: A non-arrhenian model: *American Mineralogist*, v. 81, p. 1297–1300.

Hildreth, W., 1981, Gradients in silicic magma chambers: Implications for lithospheric magmatism: *Journal of Geophysical Research*, v. 86, p. 10153–10192, doi:10.1029/JB086iB11p10153.

Huber, C., Bachmann, O., and Manga, M., 2009, Homogenization processes in silicic magma chambers by stirring and latent heat buffering: *Earth and Planetary Science Letters*, v. 283, p. 38–47, doi:10.1016/j.epsl.2009.03.029.

Huber, C., Bachmann, O., and Dufek, J., 2010a, The limitations of melting on the reactivation of silicic mushes: *Journal of Volcanology and Geothermal Research*, v. 195, p. 97–105, doi:10.1016/j.jvolgeores.2010.06.006.

Huber, C., Bachmann, O., and Manga, M., 2010b, Two competing effects of volatiles on heat transfer in crystal-rich magmas: Thermal insulation vs defrosting: *Journal of Petrology*, v. 51, p. 847–867, doi:10.1093/petrology/egq003.

Huber, C., Bachmann, O., and Dufek, J., 2011, Thermo-mechanical reactivation of locked crystal mushes: Melting-induced internal fracturing and assimilation processes in magmas: *Earth and Planetary Science Letters*, v. 304, p. 443–454, doi:10.1016/j.epsl.2011.02.022.

Lipman, P.W., 2000, The central San Juan Caldera cluster: Regional volcanic framework, in Bethke, P.M., and Hay, R.L., eds., *Ancient Lake Creede: Its volcano-tectonic setting, history of sedimentation, and relation of mineralization in the Creede mining district: Geological Society of America Special Paper 346*, p. 9–69, doi:10.1130/0-8137-2346-9.9.

Lipman P.W., 2006, *Geologic map of the central San Juan Caldera cluster, southwestern Colorado: U.S. Geological Survey Geologic Investigations Series I-2799, 4 sheets, scale 1:24,000, 37 p.*

Lipman, P.W., 2007, Incremental assembly and prolonged consolidation of Cordilleran magma chambers: Evidence from the Southern Rocky Mountain volcanic field: *Geosphere*, v.3, p. 42–70.

Marsh, B.D., 1981, On the crystallinity, probability of occurrence, and rheology of lava and magma: *Contributions to Mineralogy and Petrology*, v. 78, p. 85–98, doi:10.1007/BF00371146.

Molloy, C., Shane, P., and Nairn, I., 2008, Pre-eruption thermal rejuvenation and stirring of a partly crystalline rhyolite pluton revealed by the Earthquake Flat pyroclastic deposits, New Zealand: *Geological Society of London Journal*, v. 165, p. 435–447, doi:10.1144/0016-76492007-071.

Pallister, J.S., Hoblitt, R.P., and Reyes, A.G., 1992, A basalt trigger for the 1991 eruptions of Pinatubo volcano?: *Nature*, v. 356, p. 426–428, doi:10.1038/356426a0.

Ruprecht, P., Bergantz, G.W., and Dufek, J., 2008, Modeling of gas-driven magmatic overturn: Tracking of phenocryst dispersal and gathering during magma mixing: *Geochemistry Geophysics Geosystems*, v. 9, Q07017, doi:10.1029/2008GC002022.

Scaillet, B., Holtz, F., and Pichavant, M., 1998, Phase equilibrium constraints on the viscosity of silicic magmas 1. Volcanic-plutonic comparison: *Journal of Geophysical Research*, v. 103, no. B11, p. 27257–27266, doi:10.1029/98JB02469.

Wark, D.A., Hildreth, W., Spear, F.S., Cherniak, D.J., and Watson, E.B., 2007, Pre-eruption recharge of the Bishop magma system: *Geology*, v. 35, p. 235–238, doi:10.1130/G23316A.1.

Manuscript received 6 May 2011

Revised manuscript received 22 August 2011

Manuscript accepted 12 September 2011

Printed in USA